June 1990

Kerr effect of two-medium layered systems

Liang-Yao Chen
University of Nebraska - Lincoln

William A. McGahan
University of Nebraska - Lincoln

Z.S. Shan
University of Nebraska - Lincoln

David J. Sellmyer
University of Nebraska-Lincoln, dsellmyer@unl.edu

John A. Woollam
University of Nebraska-Lincoln, jwoollam1@unl.edu

Kerr effect of two-medium layered systems

J. Appl. Phys. -- June 15, 1990 -- Volume 67, Issue 12, pp. 7547-7555

Issue Date: June 15, 1990

Liang-Yao Chen, William A. McGahan, Z. S. Shan, D. J. Sellmyer, and John A. Woollam

Departments of Electrical Engineering and Physics, University of Nebraska, Lincoln, Nebraska 68588-0511

Detailed and practical expressions are given for the magneto-optical Kerr effect (MOKE) for various configurations of two media. One is a magneto-optic (MO) one, and the other is a nonmagnetic (NM) medium. For a system of two thick media with a single interface, with a first-order approximation in MOKE term Q, the Kerr function is determined by the product of a MOKE term Q and an optical termb η. A second type of system includes a thin MO (or NM) layer deposited on a thick NM (or MO) substrate. For a MO/(NM-substrate) configuration, the Kerr function is related to the Kerr effects from the air/MO and MO/NM interfaces, and to the Faraday effects of the MO layer, as well as to interference effects. The enhancement factor can be expected to be large by proper choice of materials. For a NM/(MO-substrate) configuration, the total Kerr function is related to the Kerr effect from the NM/MO interface and can be enhanced by interference. The enhancement factor is expected to be less than one if the NM layer is strongly absorbing. Calculations of Kerr effects for examples of the PtMnSb/$AuAl_2$ and Fe/Cu configurations are given. These indicate that the peaks shown in the onset region of the interband transitions of Cu can be attributed to a dramatic change of the refractive index in that region. The merits of a MO/(NM-metallic) structure have been evaluated, and indicate that a better Kerr enhancement effect can be achieved if the refractive index of the MO layer is larger than one and is much larger than that of the metallic material. A drawback to this configuration comes from the fact that a MO material with a large refractive index value usually is not expected to have a large intrinsic Kerr effect.

DOI: 10.1063/1.345818

Kerr effect of two-medium layered systems

Liang-Yao Chen, William A. McGahan, Z. S. Shan, D. J. Sellmyer, and John A. Woollam
Departments of Electrical Engineering and Physics, University of Nebraska, Lincoln, Nebraska 68588-0511

(Received 18 December 1989; accepted for publication 6 March 1990)

Detailed and practical expressions are given for the magneto-optical Kerr effect (MOKE) for various configurations of two media. One is a magneto-optic (MO) one, and the other is a nonmagnetic (NM) medium. For a system of two thick media with a single interface, with a first-order approximation in MOKE term Q, the Kerr function is determined by the product of a MOKE term Q and an optical term η. A second type of system includes a thin MO (or NM) layer deposited on a thick NM (or MO) substrate. For a MO/(NM-substrate) configuration, the Kerr function is related to the Kerr effects from the air/MO and MO/NM interfaces, and to the Faraday effects of the MO layer, as well as to interference effects. The enhancement factor can be expected to be large by proper choice of materials. For a NM/(MO-substrate) configuration, the total Kerr function is related to the Kerr effect from the NM/MO interface and can be enhanced by interference. The enhancement factor is expected to be less than one if the NM layer is strongly absorbing. Calculations of Kerr effects for examples of the $PtMnSb/AuAl_2$ and Fe/Cu configurations are given. These indicate that the peaks shown in the onset region of the interband transitions of Cu can be attributed to a dramatic change of the refractive index in that region. The merits of a MO/(NM-metallic) structure have been evaluated, and indicate that a better Kerr enhancement effect can be achieved if the refractive index of the MO layer is larger than one and is much larger than that of the metallic material. A drawback to this configuration comes from the fact that a MO material with a large refractive index value usually is not expected to have a large intrinsic Kerr effect.

I. INTRODUCTION

In the last two decades, considerable attention has been paid to the magneto-optical Kerr effects (MOKE) due to [illegible] cording. The Kerr parameters, rotation angle σ_k and ellipticity ϵ_k, can be directly related to both the diagonal and off-diagonal elements of the complex dielectric tensor, which is attributed not only to intraband transitions dominated by the free electrons near the Fermi surface, but also to interband transitions characterized by the joint density of states function. Intrinsically, the origin of the MOKE for ferromagnets is primarily from the "magnetic" electrons, i.e., d electrons for the transition metals and d and f electrons for the rare-earth metals. The MOKE is proportional to the product of spin-orbit coupling strength, which strongly discriminates against s-p states, and net electron polarization excited by the incident light.[1,2] Therefore, the actual physical explanation of MOKE spectra, including its enhancement, in general has traditionally been based on extensive studies of the magnetic (electronic) behavior of various magnetic materials.

Recently, however, several new mechanisms have been presented to explain the giant enhancement of the MOKE observed by different authors for a single magneto-optic (MO) or an MO/metallic bilayer film system.[3–7] Feil and Haas have shown that a resonance-shaped MOKE spectra can be induced by the plasma resonance of the free carriers of the magnetic materials.[3] Katayama *et al.* reported that for a Fe/Cu bilayer film structure the enhancement of θ_k which occurs around 2.2 eV is a result of the plasma resonance absorption of the nonmagnetic (NM) copper.[4] Reim and Weller not only demonstrated the experimental results for the TbFeCo/Cu and GdTbFeCo/Ag bilayers, but also gave an expression which shows that if the NM reflector, on which the MO thin film is deposited, has a low value of the complex refractive index an enhancement of θ_k can be ex- [illegible] ellipsometric and MOKE data to show that the resonant enhancement of θ_k for a bilayer has an optical origin. In this paper we study this problem in greater detail, but for simplicity restrict our discussion to only the polar MOKE at normal angle of incidence. The general analytical expressions and calculations are given for two types of systems, and show that although MOKE is fundamentally related to the magnetic (electronic) behavior of the material, the optical properties of both the MO and NM materials will play an equally important role in determining its value. The giant enhancement of MOKE for a MO/NM system can be explained fully from the optical origin. A complete Kerr spectrum for Fe/Cu configuration is recalculated, covering a wide spectral range, and shows that the peaks broaden and move toward longer wavelengths. They are attributed to a dramatic change of the refractive index in the onset region of the interband transitions of Cu. The merits of a MO/(NM-metallic) structure are discussed and indicate that a better enhancement effect can be achieved if the refractive index of the MO layer is larger than 1, and is much larger than that of the NM metallic material.

II. THEORY

A. Systems of two thick media with single interface

In this section we consider MOKE in two infinitely ("optically") thick media having a single interface between

 0021-8979/90/127547-09$03.00

them. The medium on top is the NM layer, and the bottom layer is the MO medium. Hereafter, this system will be denoted as (NM/MO). The simplest example is the (air/MO) configuration. But the more general case is treated here.

For a magnetized ferromagnetic material, assuming that the magnetization M is in the z direction (normal to the sample surface), a linearly polarized wave at normal angle of incidence will vibrate in the x-y plane and propagate along the z axis, respectively. The assumption of isotropy for the material implies the following form for the dielectric tensor $[\epsilon]$:[8,9]

$$[\epsilon]=\begin{bmatrix}\epsilon & \epsilon_{xy} & 0\\ -\epsilon_{xy} & \epsilon & 0\\ 0 & 0 & \epsilon_z\end{bmatrix}=\begin{bmatrix}\epsilon & -i\epsilon Q & 0\\ i\epsilon Q & \epsilon & 0\\ 0 & 0 & \epsilon_z\end{bmatrix}, \tag{1}$$

where Q is the Voigt parameter which is small and, in general, is a complex function of the magnetization of the body. The diagonal terms of the complex dielectric constant ϵ will be a weak function of Q. Since $\epsilon(Q)=\epsilon(-Q)$, the first-order term for ϵ in Q vanishes. Therefore, after omitting the terms of higher than first order in Q, ϵ can be regarded as the ordinary dielectric function related to the complex index of refraction $\tilde{n}$ as follows:

$$\epsilon=\epsilon_1+i\epsilon_2=\tilde{n}^2, \quad \text{and} \quad \tilde{n}=n+ik. \tag{2}$$

The z component of the diagonal terms of the tensor, ϵ_z, will become identical to ϵ as the magnetization goes to zero. Assuming further that the linearly polarized electric field E lies along the x axis, it can be decomposed into two circularly polarized fields, right E_r and left E_l, i.e.,

$$E_x=E_r+E_l, \tag{3}$$

where

$$E_r=\tfrac{1}{2}(E_x+iEy), \quad \text{and} \quad E_l=\tfrac{1}{2}(E_x-iEy). \tag{4}$$

If the material shows a Kerr effect, the reflected wave from the surface will be elliptically polarized. The reflected field E' is

$$E'=E'_r+E'_l=\tilde{\gamma}_+E_r+\tilde{\gamma}_-E_l, \tag{5}$$

where $\tilde{\gamma}_+$ and $\tilde{\gamma}_-$ are the reflection coefficients for right and left circularly polarized light, respectively. Now we consider in general a two-medium system, i.e., a NM medium with the complex refractive index $\tilde{n}_0$ in contact with a MO medium with the MO refractive index $\tilde{n}_\pm$. Taking the first-order approximation in Q, $\tilde{n}_\pm$ will have the following form[7,8]:

$$\tilde{n}_\pm=\tilde{n}_m(1\mp Q/2). \tag{6}$$

Assuming that the light is incident from the NM medium to the MO medium, the $\tilde{\gamma}_\pm$ will be

$$\tilde{\gamma}_\pm=\gamma_\pm e^{i\delta\pm}=\frac{\tilde{n}_0-\tilde{n}_\pm}{\tilde{n}_0+\tilde{n}_\pm}=\tilde{\gamma}\tilde{\rho}_\pm, \tag{7}$$

where $\tilde{\gamma}$ is the ordinary reflection coefficient without magnetization,

$$\tilde{\gamma}=\gamma e^{i\varphi}=\frac{\tilde{n}_0-\tilde{n}_m}{\tilde{n}_0+\tilde{n}_m}, \tag{8}$$

and $\tilde{\rho}_\pm$ is a complex quantity related to the pure MOKE. Therefore, $\tilde{\rho}_\pm$ can be solved from

$$\tilde{\rho}_\pm=\tilde{\gamma}_\pm/\tilde{\gamma}=\tilde{\rho}_\pm e^{i\theta\pm}\simeq 1+\phi_\pm=1+\epsilon_\pm+i\theta_\pm, \tag{9}$$

where $\epsilon_\pm$ and $\theta_\pm$ are small quantities related to Q. Comparing Eqs. (7)–(9), we see that

$$\gamma_\pm=\gamma\rho_\pm=\gamma(1+\epsilon_\pm), \quad \text{and} \quad \delta_\pm=\varphi+\theta_\pm. \tag{10}$$

Substituting Eqs. (6)–(8) into Eq. (9) and taking the first-order approximation in Q, we have

$$\tilde{\rho}_\pm\simeq 1\pm\eta Q, \tag{11}$$

where

$$\eta=\frac{\sqrt{\epsilon_0\epsilon_m}}{\epsilon_0-\epsilon_m}. \tag{12}$$

It is clear that

$$\phi_+=-\phi_-=\eta Q. \tag{13}$$

Finally, we obtain the Kerr parameters, ellipticity ϵ_k, and rotation angle θ_k, respectively:

$$\begin{aligned}\epsilon_k&=-\frac{\gamma_+-\gamma_-}{\gamma_++\gamma_-}=-\frac{\rho_+-\rho_-}{\rho_++\rho_-}\\ &\simeq-\epsilon_+=-\mathrm{Re}(\eta Q),\\ \theta_k&=-\frac{(\delta_+-\delta_-)}{2}=-\frac{(\theta_+-\theta_-)}{2}\\ &=-\theta_+=-\mathrm{Im}(\eta Q).\end{aligned} \tag{14}$$

Therefore, the complex Kerr function ϕ_k is

$$\phi_k=\epsilon_k+i\theta_k=-\phi_+=\frac{Q\sqrt{\epsilon_0\epsilon_m}}{\epsilon_m-\epsilon_0}=\frac{i\epsilon_{mxy}\sqrt{\epsilon_0/\epsilon_m}}{\epsilon_m-\epsilon_0}. \tag{15}$$

If the NM medium is air, $\epsilon_0=1$ and $\epsilon_m=\epsilon$, and we have the same expression for $\tilde{\phi}_k$ as given by other authors[3,10]:

$$\phi_{k0}=\frac{Q\sqrt{\epsilon}}{\epsilon-1}=\frac{i\epsilon_{xy}}{\sqrt{\epsilon}(\epsilon-1)}. \tag{16}$$

Equation (15) was derived assuming $\phi_\pm\ll 1$ in Eqs. (9) and only the first-order approximation in Q was taken into account. It is interesting to see what will happen if the optical constants of the two media are nearly the same. Assuming $\tilde{n}_0\simeq\tilde{n}_m$, Eqs. (6), (7), and (14) yield

$$\gamma_\pm\simeq\pm\frac{Q}{4}=\pm\frac{|Q|}{4}e^{i\delta}, \tag{17}$$

and thus $\epsilon_k=0$, and $\theta_k=\pi/2$. The reflectivity R is

$$R=\frac{1}{2}(|\gamma_+|^2+|\gamma_-|^2)\simeq\frac{|Q|^2}{16}. \tag{18}$$

It is clear that the reflected light is linearly polarized, but the direction of the electric field has been rotated by 90° and has a low intensity.

It can also be shown that if the light is incident from the MO media to the NM media, ϕ_k will be unchanged and have the same form as Eq. (15).

Finally, assuming that both media are ferromagnetic and have the Voigt parameters Q_0 and Q_m, respectively, the Kerr function can be shown to be

$$\phi_k=\frac{(Q_m-Q_0)\sqrt{\epsilon_0\epsilon_m}}{\epsilon_m-\epsilon_0}=i\frac{(\epsilon_0\epsilon_{mxy}-\epsilon_m\epsilon_{oxy})}{(\epsilon_m-\epsilon_0)\sqrt{\epsilon_0\epsilon_m}}. \tag{19}$$

The Kerr effect will be enhanced when Q_0 and Q_m have opposite signs, and weakened when they have the same signs.

B. Layered systems with one thin medium

1. MO/(NM-substrate) configurations

Assume that a MO layer, with a complex refractive index $n_\pm$ and layer thickness d, lies on top of an infinitely thick NM substrate having a complex refractive index $\tilde{n}_0$. Hereafter, this configuration will be denoted as [MO/NM]. As shown in part (a) of Fig. 1, the reflection coefficients $\tilde{\gamma}'_\pm$ of right and left circularly polarized light for the [MO/NM] system at wavelength λ will be

$$\tilde{\gamma}'_\pm = \gamma'_\pm e^{i\delta'_\pm} = \frac{\tilde{\gamma}_{\pm 1} + \tilde{\gamma}_{\pm 2} e^{i\beta_\pm}}{1 + \tilde{\gamma}_{\pm 1}\tilde{\gamma}_{\pm 2} e^{i\beta_\pm}}, \tag{20}$$

where

$$\begin{aligned}
&\tilde{\gamma}_{\pm 1} = \frac{1 - \tilde{n}_\pm}{1 + \tilde{n}_\pm} = \tilde{\gamma}_1 \tilde{\rho}_{\pm 1}, \\
&\tilde{\gamma}_{\pm 2} = \frac{\tilde{n}_\pm - \tilde{n}_0}{\tilde{n}_\pm + \tilde{n}_0} = \tilde{\gamma}_2 \tilde{\rho}_{\pm 2}, \\
&\beta_\pm = 4\pi \tilde{n}_\pm d/\lambda = \beta + \chi_\pm,
\end{aligned} \tag{21}$$

with

$$\begin{aligned}
&\tilde{\gamma}_1 = \frac{1 - \tilde{n}_m}{1 + \tilde{n}_m}, \quad \text{and} \quad \tilde{\gamma}_2 = \frac{\tilde{n}_m - \tilde{n}_0}{\tilde{n}_m + \tilde{n}_0}, \\
&\tilde{\rho}_{\pm 1} = 1 + \phi_{\pm 1}, \quad \text{and} \quad \tilde{\rho}_{\pm 2} = 1 + \phi_{\pm 2}, \\
&\beta = 4\pi \tilde{n}_m d/\lambda, \quad \text{and} \quad \chi_\pm = \mp 2\pi \tilde{n}_m Q d/\lambda.
\end{aligned} \tag{22}$$

Therefore, considering the first-order approximation in Q, and Eq. (20) will be

$$\tilde{\gamma}'_\pm = \tilde{\gamma}'(1 + \phi'_\pm) = \tilde{\gamma}'(1 + \epsilon'_\pm + i\theta'_\pm), \tag{23}$$

where $\tilde{\gamma}'$ is the ordinary reflection coefficient for the [MO/NM] configuration:

$$\tilde{\gamma}' = \frac{\tilde{\gamma}_1 + \tilde{\gamma}_2 e^{i\beta}}{1 + \tilde{\gamma}_1 \tilde{\gamma}_2 e^{i\beta}}. \tag{24}$$

In the same way as mentioned above, the Kerr function ϕ'_k for such an [MO/NM] configuration is then

$$\begin{aligned}
\phi'_k &= \epsilon'_k + i\theta'_k = -\phi'_+ \\
&= \frac{(1 - \tilde{\gamma}_2^2 e^{i2\beta})\tilde{\gamma}_1 \phi_{k1} + (1 - \tilde{\gamma}_1^2)(\phi_{k2} + 2\phi_F)\tilde{\gamma}_2 e^{i\beta}}{(\tilde{\gamma}_1 + \tilde{\gamma}_2 e^{i\beta})(1 + \tilde{\gamma}_1 \tilde{\gamma}_2 e^{i\beta})},
\end{aligned} \tag{25}$$

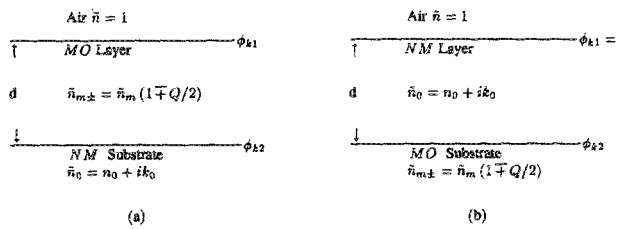

FIG. 1. Thin layered configurations: (a) the MO layer lies on top of the NM substrate, (b) the NM layer lies on top of the MO substrate.

where $\phi_{k1} = \phi_{k0}$ in Eq. (16), and $\phi_{k2} = \phi_k$ in Eq. (15). These are the Kerr functions related to the air/MO and MO/NM interfaces, respectively, and ϕ_F is the Faraday function related to the Faraday ellipticity ϵ_F and rotation θ_F[10]:

$$\phi_F = \epsilon_F + i\theta_F = i|\chi_\pm|/2. \tag{26}$$

It can be seen that as $d \to 0$, $\phi_k' \to 0$, and as $d \to \infty$ and $k_m \neq 0$, $\phi'_k \to \phi_{k1}$. Equation (25) is also suitable to a [MO/MO] configuration with $\phi_{k2} = \phi_k$ in Eq. (19), and valid when

$$\begin{aligned}
&\frac{\tilde{\gamma}_1 \tilde{\gamma}_2 e^{i\beta}(\phi_{k1} + \phi_{k2} + 2\phi_F)}{1 + \tilde{\gamma}_1 \tilde{\gamma}_2 e^{i\beta}} \ll 1, \\
&\frac{\tilde{\gamma}_1 \phi_{k1} + (\phi_{k2} + 2\phi_F)\tilde{\gamma}_2 e^{i\beta}}{(\tilde{\gamma}_1 + \tilde{\gamma}_2 e^{i\beta})} \ll 1.
\end{aligned} \tag{27}$$

2. NM/(MO-substrate) configurations

For the system in which a NM layer lies on top of the MO substrate, denoted as [NM/MO], which has the configuration shown in part (b) of Fig. 1, the Kerr function ϕ'_k will be modified to

$$\phi'_k = \frac{\tilde{\gamma}_2(1 - \tilde{\gamma}_1^2)\phi_{k2} e^{i\beta}}{(\tilde{\gamma}_1 + \tilde{\gamma}_2 e^{i\beta})(1 + \tilde{\gamma}_1 \tilde{\gamma}_2 e^{i\beta})}, \tag{28}$$

where

$$\begin{aligned}
&\tilde{\gamma}_1 = \frac{1 - \tilde{n}_0}{1 + \tilde{n}_0}, \quad \text{and} \quad \tilde{\gamma}_2 = \frac{\tilde{n}_0 - \tilde{n}_m}{\tilde{n}_0 + \tilde{n}_m}, \\
&\beta = 4\pi \tilde{n}_0 d/\lambda.
\end{aligned} \tag{29}$$

As $d \to 0$, $\phi'_k \to \phi_{k1}$, and as $d \to \infty$ and $k_0 \neq 0$, $\phi'_k \to 0$.

III. DISCUSSION

A. Physical origins of Kerr effects

The off-diagonal element of the complex dielectric tensor, ϵ_{xy}, contains contributions from both intraband and interband transitions. In the near-infrared and visible photon energy region, the intraband part of ϵ_{xy} can be approximated as[11]

$$\epsilon_{xy} = \epsilon_{xy1} + i\epsilon_{xy2} = \frac{i4\pi\sigma_{xy}}{\omega} \simeq -if_p \frac{\omega_p^2}{\omega(1 + i\omega\tau)}, \tag{30}$$

where f_p is the function related to the dipole moment and spin polarization of the magnetic electrons. The interband transitions play an important role in ϵ_{xy} when photon energies match the energy-band gaps. The absorptive and dispersive parts, ϵ_{xy1} and ϵ_{xy2}, of ϵ_{xy} from the interband effect can be given, respectively, with the Kramers–Kronig relation[11]

$$\begin{aligned}
&\epsilon_{xy1} = -\frac{\pi^2 e^2}{\hbar\omega^2 m^2} \overline{F}_{\alpha\beta}(\omega) J_{\alpha\beta}(\omega), \\
&\epsilon_{xy2} = \frac{2}{\pi} P \int \frac{\omega' \epsilon_{xy1}}{(\omega'^2 - \omega^2)} d\omega',
\end{aligned} \tag{31}$$

where $\overline{F}_{\alpha\beta}(\omega)$ is a combined matrix element of the kinetic-momentum and spin-orbit operators, and $J_{\alpha\beta}(\omega)$ is the ordinary function of the joint density of states (JDOS):

$$J_{\alpha\beta}(\omega)=\frac{1}{(2\pi)^3}\int \delta(\omega_{\alpha\beta}-\omega)d^3k\,. \tag{32}$$

The form of $i\epsilon_{xy}$ thus is quite similar to that of the diagonal term ϵ, except for the difference in the formation of the matrix elements.

The energy loss by the collective movement of electrons in the solid is proportional to the loss function $\mathrm{Im}(-1/\epsilon)$ for creation of volume excitations and $\mathrm{Im}[-1/(\epsilon+1)]$ for creation of surface excitations.[12] At the plasma edge, a loss maximum will usually occur, as ϵ_2 is small and $\epsilon_1 \simeq 0$ and -1 for the volume, and surface energy-loss functions, respectively.

Therefore, for an ideal (NM/MO) configuration, according to Eq. (15), four physical quantities in general will contribute to the Kerr function ϕ_k: (1) ϵ_{mxy}, which has its origins in intraband and interband transitions in the MO material and usually shows structure when the photon energies are equal to the band gaps. (2) $1/\sqrt{\epsilon_m}$, which has features similar to the energy-loss function at the plasma edge, but notice that in general ϵ_m is not totally independent of ϵ_{mxy}. Hence, if ϵ_m has a strong correlation to ϵ_{mxy}, the effect from this term will be partly canceled. (3) The optical matching term $1/(\epsilon_m-\epsilon_0)$ for which maxima occur as $\epsilon_m \simeq \epsilon_0$. (4) $\sqrt{\epsilon_0}$, or $\tilde{n}_0$, which are related to the optical properties of the NM medium. It is clear that a small ϵ_0, corresponding to a plasmon of the NM medium, will not contribute to the enhancement of the Kerr effect, unless it matches ϵ_m.

B. Application to (air/PtMnSb) configuration

We take again the MO material PtMnSb as an example,[3,13,14] and consider that the NM medium is air, $\epsilon_0=1$, and $\epsilon_m=\epsilon$. The diagonal ϵ and off-diagonal ϵ_{xy} terms of the dielectric tensor, the loss function $\mathrm{Im}(-1/\epsilon)$, and the optical matching term $1/(\epsilon-1)$, as well as the Kerr function for (air/PtMnSb) are shown in Figs. 2–6, respectively. van der Heide *et al.*[14] experimentally determined that the onset of interband transitions for PtMnSb is at about 0.9 eV, at the tail of the photoconductivity σ curve. However, by means of least-squares fitting to the linear part of $\epsilon_2(\hbar\omega)^2$, or $\omega\sigma$, which is proportional to JDOS (see Fig. 7), the onset of the interband transitions for PtMnSb can be determined to be at about 1.6 eV. The same absorptive tail features were observed for other materials such as Au[15,16] and $AuAl_2$.[17] The sharp peak at 1.68 eV in the loss function, as seen in Fig. 4, is attributed to a plasmon ($\epsilon_1=0$ at 1.66 eV) being shifted in energy ($\hbar\omega_p=6.1$eV) due to the effect of the interband transitions. The absorptive part of the off-diagonal dielectric tensor, ϵ_{xyI}, shows a sharp peak at about 1.54 eV, which is shifted to 1.6 eV in $\epsilon_{xyI}(\hbar\omega)^2$, as seen in Figs. 3 and 7. This peak has the same origin that is the onset of interband transitions, but is associated with the spin-orbit interaction characterized by the matrix element $\bar{F}_{\alpha\beta}$. The energy-band calculation[18] (made using a self-consistent augmented spherical wave method) indicated that the onset of a strong MO absorption occurs at the Γ point at the 1.2-eV photon energy, which arises from the minority-spin-band Γ_4 $(m=1)$ $\rightarrow\Gamma_1$ $(m=0)$ transition and is qualitatively in agreement

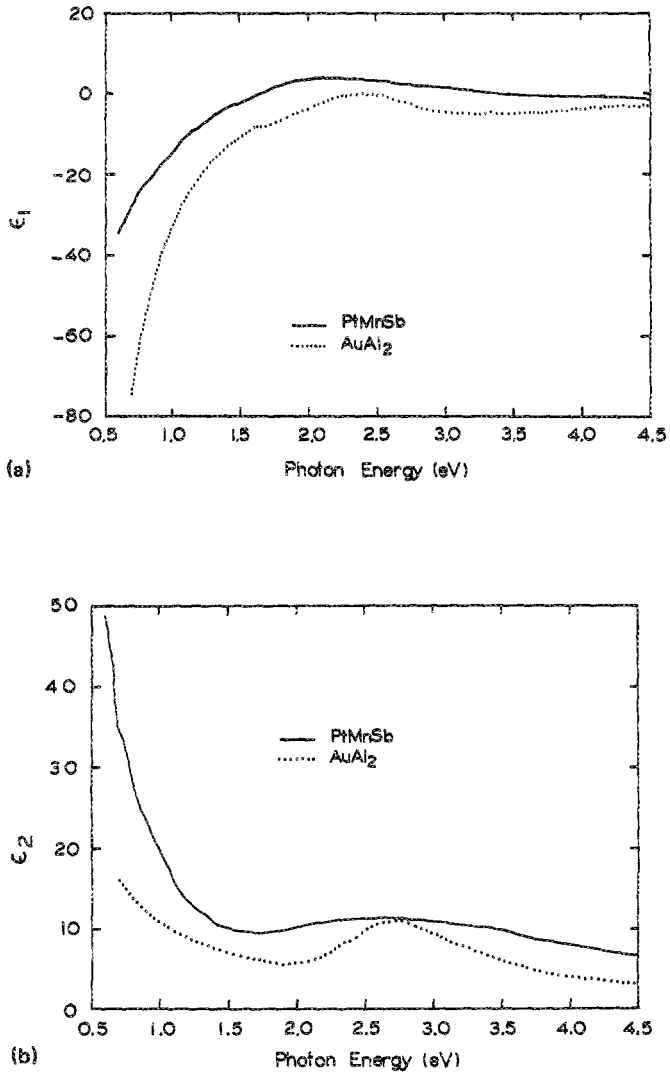

FIG. 2. Complex dielectric functions of PtMnSb and $AuAl_2$ from Refs. 14 and 17.

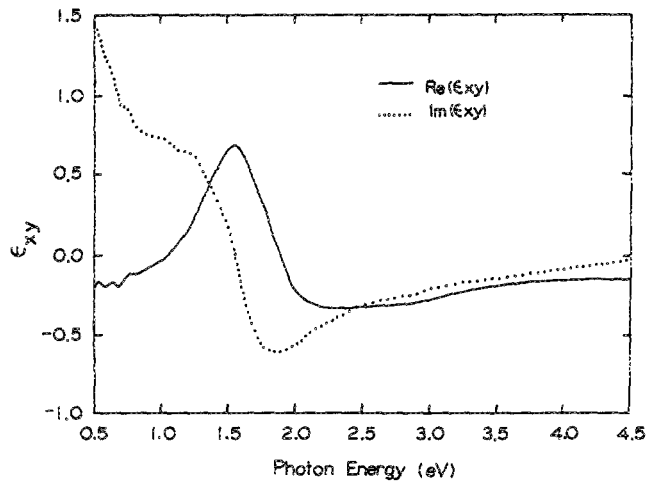

FIG. 3. Off-diagonal terms of the dielectric tensor of PtMnSb, calculated from Refs. 13 and 14.

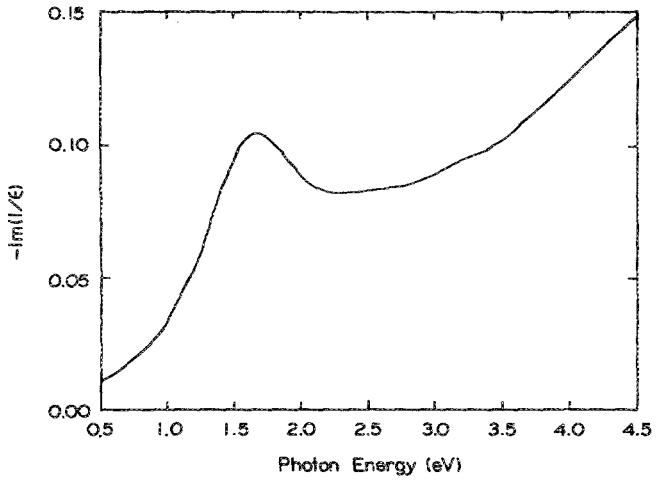

FIG. 4. Loss function of PtMnSb, calculated from Ref. 14.

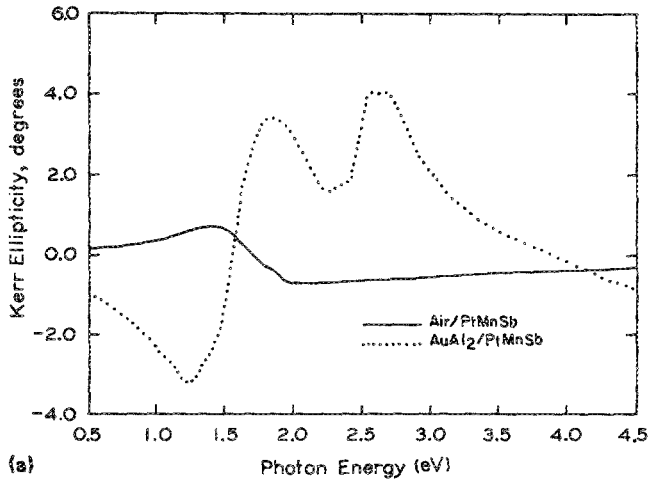

with the experimental results.[13,14] The optical matching term $1/(\epsilon - 1)$ shows one peak at about 1.7 eV in the imaginary part, and two broad peaks at about 1.4 and 2.1 eV in the real part, as seen in Fig. 5. The combined effects of the three physical quantities finally predict a single resonantlike peak at around 1.7 eV in the Kerr rotation spectrum, as seen in Fig. 6.

C. Application to ($AuAl_2$/PtMnSb) configuration

Now we replace air with, for example, $AuAl_2$,[17] i.e., assume a ($AuAl_2$/PtMnSb) configuration. The dielectric functions of $AuAl_2$ as well as PtMnSb are shown in Fig. 2. Using Eq. (15), the calculated Kerr function of ($AuAl_2$/PtMnSb) with comparison to (air/PtMnSb) is shown in Fig. 6. It is obvious that the first strong peak in the Kerr effect of ($AuAl_2$/PtMnSb) in the 1–2-eV photon energy range comes primarily from the contributions of ϵ_{mxy} and $1/\sqrt{\epsilon_m}$ of PtMnSb and, weakly, from optical matching. However, the second strong peak around 2.5 eV is purely from optical matching and is dominated by $1/(\epsilon_m - \epsilon_0)$, as

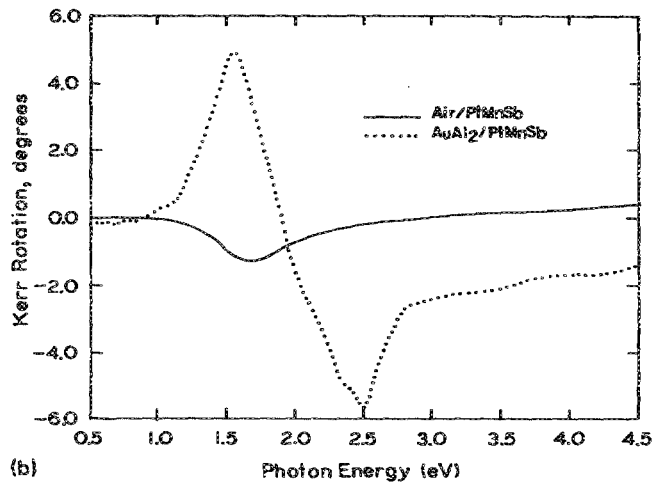

FIG. 6. Comparisons of the Kerr effects between the (air/PtMnSb) and ($AuAl_2$/PtMnSb) configurations.

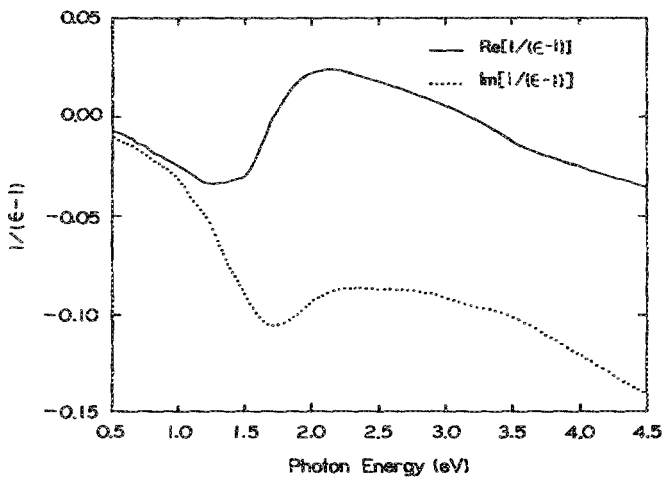

FIG. 5. Calculated optical matching term, $1/(\epsilon - 1)$, for (air/PtMnSb) structure.

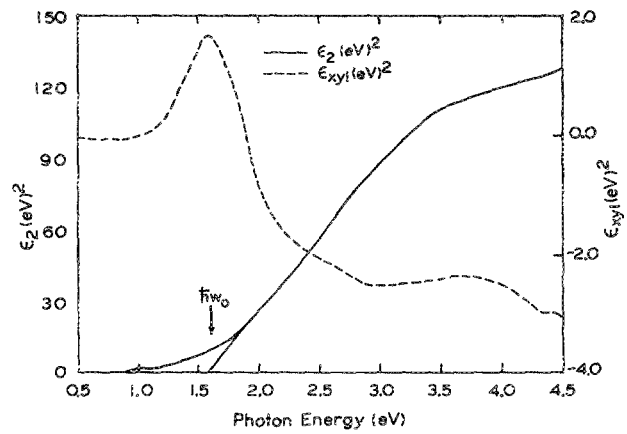

FIG. 7. Functions of the joint density of state of PtMnSb, which is proportional to $(\hbar\omega)^2\epsilon_2$, or $(\hbar\omega)^2\epsilon_{xy1}$, and calculated from Refs. 13 and 14. A linearity can be seen clearly at the onset of interband transitions in $(\hbar\omega)^2\epsilon_2$.

seen in Fig. 8. The plasma resonance of nonmagnetic $AuAl_2$ occurs at 2.1 eV[17] and clearly makes no contribution to the enhancement of the Kerr effect of ($AuAl_2$/PtMnSb).

D. Practical geometries

In practical geometries, the Kerr effect for [MO/NM] and [NM/MO] configurations, i.e., an optically thin layer lies on a substrate of the other kind of material, is given by Eqs. (25) and (28), respectively. For a [MO/NM] structure, each term in Eq. (25) has clear physical meaning. ϕ_{k1} and ϕ_{k2} present the Kerr effects occurred at the first air/MO and the second MO/NM interfaces, respectively. $2\phi_F$ originates from the Faraday effect as the light travels back and forth in the MO layer. $\tilde{\gamma}$ and β represent the magnitude and interference aspects of the reflected light, respectively. If we let

$$\tilde{\alpha}_1 = \alpha_1 e^{i\Delta_1} = \tilde{\gamma}_2/\tilde{\gamma}_1,$$
$$\tilde{\alpha}_2 = \alpha_2 e^{i\Delta_2} = (\phi_{k2} + 2\phi_F)/\phi_{k1}\,, \tag{33}$$
$$\beta_1 = 4\pi n_m d/\lambda, \quad \text{and} \quad \beta_2 = 4\pi k_m d/\lambda,$$

then Eq. (25) can be written as

$$\phi_k' = \phi_{k1}\zeta\,, \tag{34}$$

where ζ is the enhancement factor, and if $\tilde{\gamma}^2 \ll 1$,

$$\zeta = \frac{(1-\tilde{\gamma}_2^2 e^{i2\beta}) + (1-\tilde{\gamma}_1^2)\mu e^{i\nu}}{(1+\tilde{\alpha}_1 e^{i\beta})(1+\tilde{\gamma}_1\tilde{\gamma}_2 e^{i\beta})} \simeq \frac{1+\mu e^{i\nu}}{(1+\tilde{\alpha}_1 e^{i\beta})}, \tag{35}$$

and with

$$\mu = \alpha_1\alpha_2 e^{-\beta_2}, \quad \text{and} \quad \nu = \Delta_1 + \Delta_2 + \beta_1\,. \tag{36}$$

Therefore, in order to cause an enhancement, either the denominator of Eq. (35) goes to a minimum (this is a strong interference condition: $\Delta_1 + \beta_1 = m\pi$, with $m = 1,3,5,...$, which will cause a reduction in reflectivity), or the numerator has a maximum (which implies that μ should be larger with $\nu = 2m\pi$, $m = 0,1,2,...$). For properly choosing the materials, without strong interference ζ still can be larger than one.

For a [NM/MO] configuration, the top layer is non magnetic, and so $\phi_F = 0$, and only the NM/MO interface will contribute to the Kerr effect. Let

$$\tilde{\alpha}_2 = \alpha_2 e^{i\Delta_2} = \phi_{k2}/\phi_{k1}, \ \beta_1 = 4\pi n_0 d/\lambda,$$

and

$$\beta_2 = 4\pi k_0 d/\lambda, \tag{37}$$

then from Eq. (28) the enhancement factor ζ is

$$\zeta = \frac{(1-\tilde{\gamma}_1^2)\mu e^{i\nu}}{(1+\tilde{\alpha}_1 e^{i\beta})(1+\tilde{\gamma}_1\tilde{\gamma}_2 e^{i\beta})} \simeq \frac{\mu e^{i\nu}}{(1+\tilde{\alpha}_1 e^{i\beta})}, \tag{38}$$

where μ and ν are defined by Eq. (36). It is clear that if the layer is strongly absorbing, without interference ($\Delta_1 + \beta_1 = m\pi$, with $m = 1,3,5,...$), usually ζ will be less than one, since the numerator is dominated by $e^{-\beta_2}$.

When strong interferences occur, there is possibly a sign change for $\phi'_{k_{max}}$ depending on if $\alpha_1 e^{-\beta_2}$ in Eqs. (35) and (38) is less or larger than one.

Using Eqs. (25) and (28), we calculate the Kerr effects for the [PtMnSb/$AuAl_2$] and [$AuAl_2$/PtMnSb] configurations with varied layer thicknesses. The results are shown in Figs. 9 and 10. The calculated Kerr effects are enhanced in [PtMnSb/$AuAl_2$] but weakened in [$AuAl_2$/PtMnSb], and

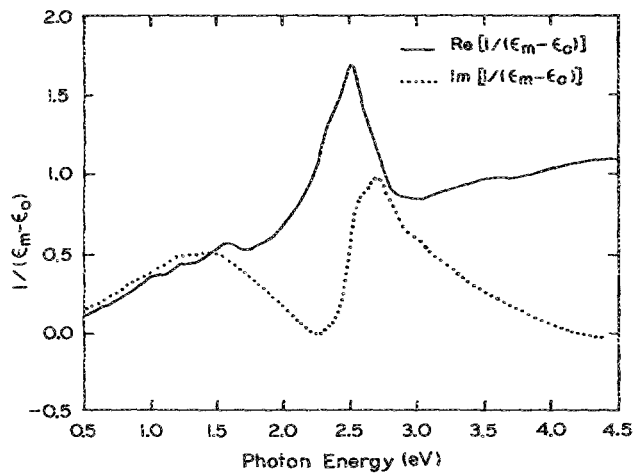

FIG. 8. Calculated optical matching term, $1/(\epsilon_m - \epsilon_0)$, for a ($AuAl_2$/PtMnSb) configuration.

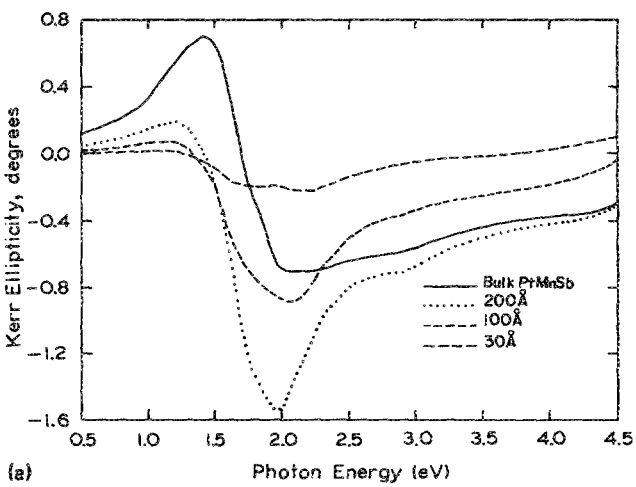

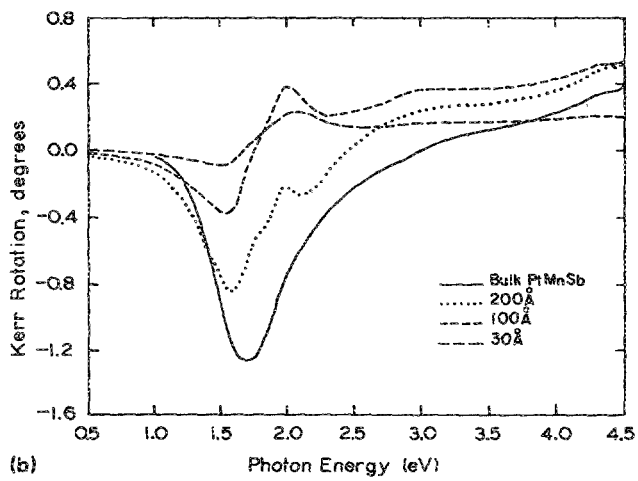

FIG. 9. Calculated Kerr effect for a [PtMnSb/$AuAl_2$] configuration.

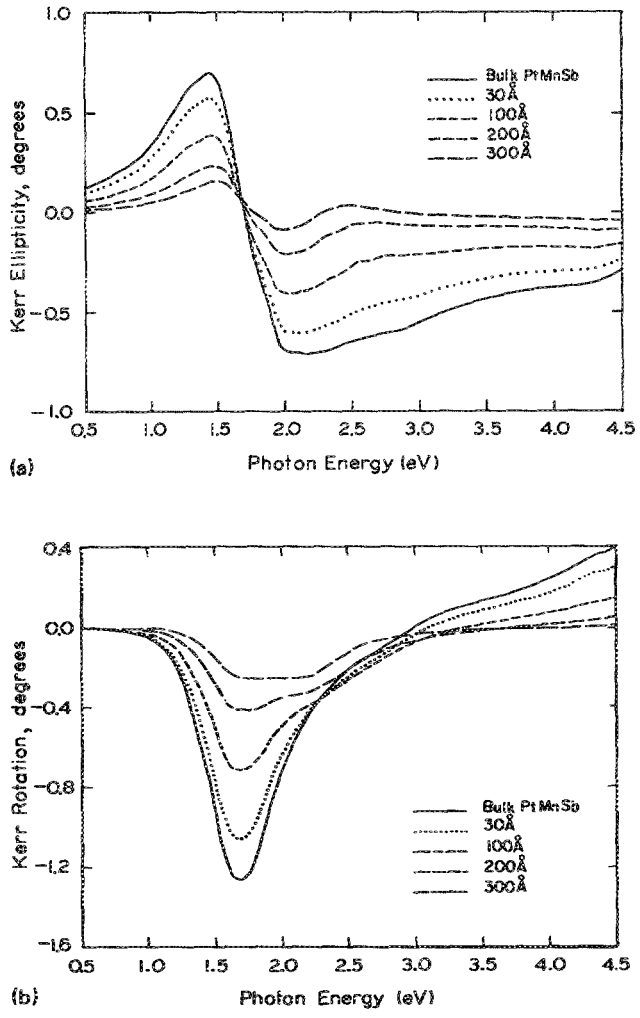

FIG. 10. Calculated Kerr effect for a [$AuAl_2$/PtMnSb] configuration.

are in agreement with the predictions discussed above. Now compare the Kerr effect for thin film versus the ideal thick ($PtMnSb/AuAl_2$) system as shown in Fig. 6: The second peak around 2.5 eV caused by optical matching effect disappears. This is due to the terms of $\tilde{\gamma}_1\phi_{k1}$ and $\tilde{\gamma}\phi_{k2}$ in Eqs. (25) and (28) which mainly cancel the optical matching effect. $\tilde{\gamma}\phi_k$, $\propto\sqrt{R}\,\phi_k$, is a quantity being used to evaluate the signal-to-noise ratio since ϕ_K is small[19]; then from Eqs. (8) and (15),

$$\tilde{\gamma}\phi_k = \pm\frac{Q\tilde{n}_0\tilde{n}_m}{(\tilde{n}_0+\tilde{n}_m)^2} = \pm\frac{i\epsilon_{mxy}\tilde{n}_0}{\tilde{n}_m(\tilde{n}_0+\tilde{n}_m)^2}. \tag{39}$$

Although using $\tilde{n}_0$ as a variable, a maximum in $\tilde{\gamma}\phi_k$ can be found that $(\tilde{\gamma}\phi_k)_{\max} = \pm 0.25Q$ as $\tilde{n}_0 = \tilde{n}_m$, the effect is obviously much weaker than that due to $1/(\epsilon_m - \epsilon_0)$ enhancement.

The ratio of $\tilde{\gamma}'\phi_k'$ to $\tilde{\gamma}_1\phi_{k1}$ and ξ, which in the first-order approximation is independent of Q, can be used to evaluate the merits of a thin layered structure. For the [MO/NM] configuration, using Eqs. (24) and (25),

$$\xi = \frac{\tilde{\gamma}'\phi_k'}{\tilde{\gamma}_1\phi_{k1}} = \frac{(1-\tilde{\gamma}_2^2e^{i2\beta})+(1-\tilde{\gamma}_1^2)\mu e^{i\nu}}{(1+\tilde{\gamma}_1\tilde{\gamma}_2e^{i\beta})^2} \simeq 1+\mu e^{i\nu}, \tag{40}$$

and for the [NM/MO] configuration, using Eq. (28),

$$\xi = \frac{\tilde{\gamma}'\phi_k'}{\tilde{\gamma}_1\phi_{k1}} = \frac{(1-\tilde{\gamma}_1^2)\mu e^{i\nu}}{(1+\tilde{\gamma}_1\tilde{\gamma}_2e^{i\beta})^2} \simeq \mu e^{i\nu}. \tag{41}$$

E. Application of theory for finite thick layers to Fe/Cu and other systems

As a final example, we use published data[20–22] and Eqs. (25) and (28) to calculate the Kerr effects for the thin layered [Fe/Cu] and [Cu/Fe] structures. These are shown in Figs. 11 and 12, respectively. The calculated Kerr rotation for the [Fe/Cu] is in agreement with the Katayama *et al.*[4] results, but our calculations were done in a wider spectral range and show clearly that the peaks in the Kerr rotation broaden and move toward longer wavelengths for the thicker layers. The same phenomena also have been observed for the layered [DyCo/Ag] configurations.[6,7] Differences between the experimental data and calculations for the [MO/NM] and [NM/MO] structures are usually due to uncertainties in the optical constants of thin layers. This is caused by defects in thin layers, as thicknesses are on the order of 100–200 Å. Other problems are the oxidization of

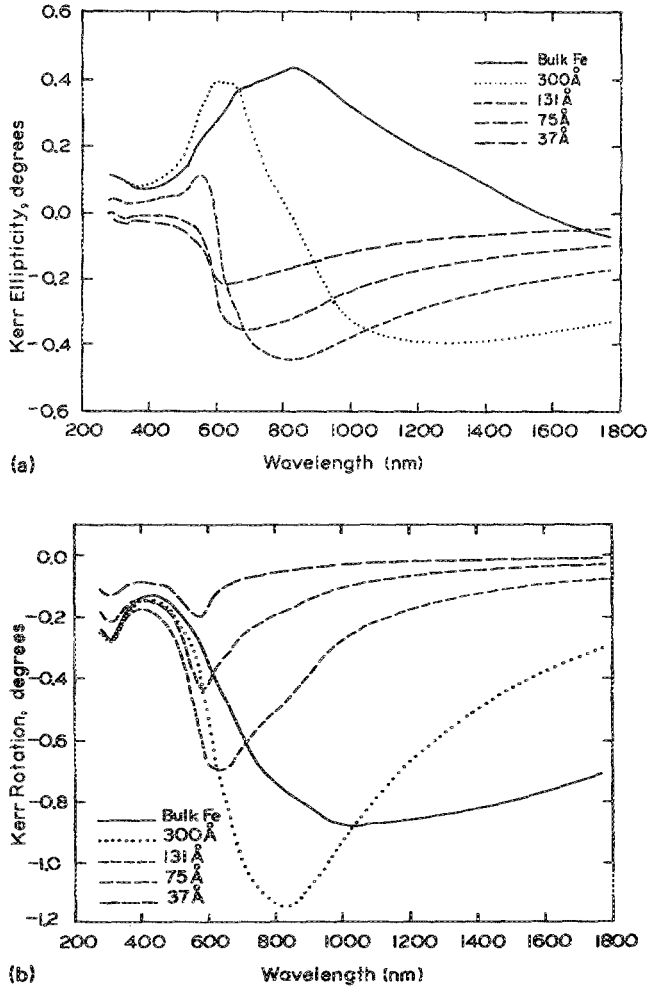

FIG. 11. Calculated Kerr effect for a [Fe/Cu] configuration.

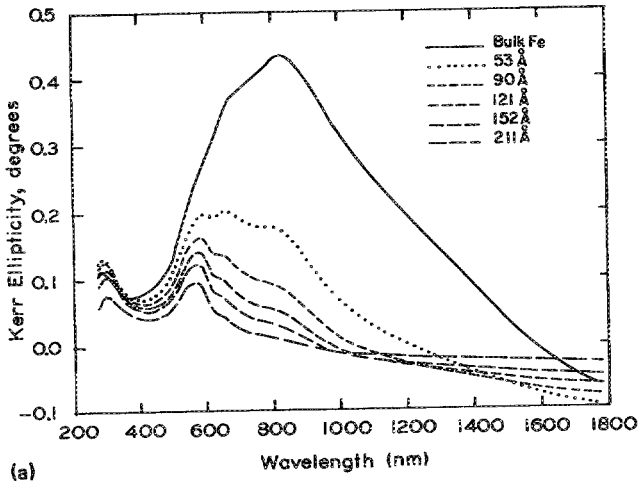

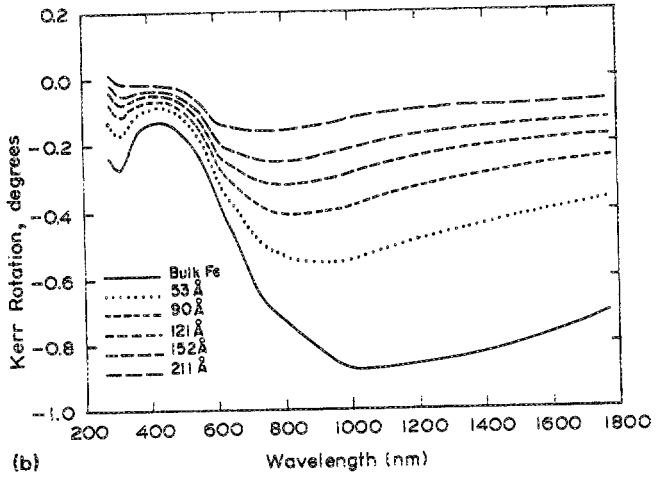

FIG. 12. Calculated Kerr effect for a [Cu/Fe] configuration.

the samples or, even in some situations, the low-dimensionality effects as layers are only a few monolayers thick.[23–27] The peaks around 5600 Å (~2.2 eV) are present for both the [Fe/Cu] and [Cu/Fe] configurations as seen in Figs. 11 and 12. We have carefully checked each term in Eqs. (25) and (28), and found that the peaks indeed originate from a dramatic change of the refractive index n_0 of Cu in the 1.9–2.5-eV photon energy region (k_0 is large but n_0 changes from 0.2 to 12.), where the onset of the interband transitions from the filled d bands to the sp conduction bands occurs. Although noble metals, Au, Ag, and Cu all show the same features of a dramatic change of the refractive index in the onset region of the interband transitions, only Ag possesses a complete plasma effect in that region where $\epsilon_1 = 0$ and ϵ_2 is small.[21,28–30]

For a [MO/NM] system where NM is metallic, Reim and Weller[5] suggested that the low values of the refractive index of the metallic reflector could lead to an enhancement of the MOKE. However, the equations they used are only suited to the interface of air/MO, not to that of MO/metallic structures. From Eqs. (22) and (40), in order to achieve a large ξ (the ratio of $\tilde{\gamma}'\phi_k'$ to $\tilde{\gamma}_1\phi_{k1}$), the denominator should be small. This implies (1) that $\tilde{n}_m < 1$ and $\tilde{n}_m \ll \tilde{n}_0$, which is unrealistic for most ferromagnetic materials and will also result in a small value of the numerator to cancel the effect, or (2) that $\tilde{n}_m > 1$ and $\tilde{n}_m \gg \tilde{n}_0$ with adjustable layer thicknesses. The latter is possible. The physical meaning of using $\tilde{n}_m \gg \tilde{n}_0$ to enhance the Kerr effect is that the reflection coefficient $\tilde{\gamma}_2$ is ~1, which results in a near-zero Kerr effect for the second MO/metallic interface, as indicated by Eq. (15). This will allow more multiple reflections and increase the influence of the Faraday effect in the MO layer, since there is no energy loss at the MO/metallic interface. The best reflector is Ag, which has the lowest value of $\tilde{n}_0$ in the visible range, $n_0 = 0.53$ and $k_0 = 0.40$ at the 3.77-eV photon energy, the plasma edge.[31] The maximum n_m and k_m values for most transition metals are less than 3 near the 3.75-eV photon energy. Thus, using Ag as a reflector, the best results can be estimated to occur when $|\xi_{\max}| \sim 2$ with thickness $d \sim 60$ Å for most [MO/Ag] configurations. In some cases, although the metallic material has a plasmon, if $\tilde{n}_m$ is not much larger than $\tilde{n}_0$, the Kerr effect will not be significantly enhanced, as seen for the situation of the [PtMnSb/$AuAl_2$] structure, in which $AuAl_2$ has a plasmon at ~2.1 eV, the Kerr effect hardly shows an enhancement in that photon energy range, as seen in Fig. 9. As for the reflectors such as Au, Cu, or other elemental metals, the enhancement effect can be expected to be worse than when using Ag which has the largest ratio of $\tilde{n}_m$ to $\tilde{n}_0$ (in the visible range) of most transition metals.

Comparisons of the enhancement effects for reflectors using Ag, Au, Cu, and Sn have been given by Reim and Weller,[32] and show agreement with our results. The reason Ag has a small refractive index at the absorption edge is that the 4-d band of Ag lies about 4 eV below the Fermi level, and thus the Drude tail is relatively far from the interband transition region and has a very small value in that region. For Au and Cu, the Drude tails are very close to the absorption edges which are at ~2.5 eV for Au and ~2.2 eV for Cu, respectively. Thus the Drude terms are still large as the tails reach these spectral regions. Therefore, for pursuing a small refractive index value in the near-infrared and visible region, the Drude parameters, such as the plasma frequency ω_p and scattering rate $1/\tau$ of the metallic reflector, should be small, and the band gap should be larger than about 3 or 4 eV.

For practical applications, there is little hope for finding small refractive index values in the 1–3-eV range using the noble metals, which all have a high number of the free electrons. However, this will be possible for the transition-metal-based compounds. After alloying with a transition metal, a part of the valence electrons from other elements will possibly fill the originally unfilled d band of the transition metal, and thus push the d band below the Fermi level. Meanwhile the compound has a smaller number of free electrons, which makes the plasma frequency lower.

On the other hand, according to Eq. (16), a MO material possessing a larger refractive index value intrinsically will not be expected to have a large intrinsic Kerr effect. If Eq. (16) is rewritten as

$$\phi_{k0} = ig\epsilon_{xy}\,, \tag{42}$$

where g is an optical term related to the intrinsic Kerr effect:

$$g = \frac{1}{\tilde{n}_m(\tilde{n}_m^2 - 1)}, \tag{43}$$

and also hypothetically assuming that all MO materials have the same value of ϵ_{xy}, then $g\xi$ can be used to evaluate the relative merits of [MO/NM] systems. It is clear that the MO material which has a larger intrinsic Kerr effect even with a smaller $\tilde{n}_m$ (but still keeping $\tilde{n}_m/\tilde{n}_0 \gg 1$) is better, although the enhancement effects are somewhat weakened.

IV. CONCLUSION

Details of the general expressions for the magneto-optical polar Kerr effect for several configurations of MO and NM media have been worked out. For a (MO/NM) system, with a first-order approximation in Q, the Kerr function is actually determined by the product of a MOKE term Q and an optical term η, as seen in Eq. (15). A plasmon from the MO material will enhance the Kerr effect, if the plasmon is not strongly correlated to ϵ_{xy}; otherwise the effect would be partly canceled. But a plasmon from the NM material will weaken the Kerr effect for this sytem. Especially for an (air/MO) system, an enhancement of the Kerr effect by a plasmon will always be assoicated with a dramatic drop in reflectivity. For a [MO/NM] configuration, the Kerr function is related not only to the Kerr effects from the air/MO and MO/NM interfaces, but also to the Faraday effect of the MO layer, as well as to the interference strength. The enhancement factor can be expected to be larger than 1 for properly chosen materials. For a [NM/MO] configuration, the Kerr function is related only to the Kerr effect from the NM/MO interface coupled with the interference effect, and the enhancement factor will usually be expected to be less than one if the NM layer is strongly absorbing.

Calculations of the Kerr effects for examples of the [PtMnSb/$AuAl_2$] and [Fe/Cu] configurations are also given, and indicate that the peaks found in the onset region of the interband transitions of Cu are actually attributed to a dramatic change of the refractive index in that region. The merits of a [MO/NM] structure have been evaluated by calculating the ratio of $\tilde{\gamma}'\phi_k'$ to $\tilde{\gamma}\phi_{k1}$ and indicate that a better enhancement effect can be achieved if the refractive index of the MO layer is larger than 1 and much larger than that of the NM metallic material. A drawback will also be associated with the fact that a MO material with a large refractive index value will usually not be expected to have a large intrinsic Kerr effect.

ACKNOWLEDGMENT

This work was supported by National Science Foundation (NSF) Grant No. DMR 8605367.

[1] P. S. Pershan, J. Appl. Phys. **38**, 1482 (1967).
[2] J. L. Erskine and E. A. Stern, Phys. Rev. Lett. **30**, 1329 (1973).
[3] H. Feil and C. Haas, Phys. Rev. Lett. **58**, 65 (1987).
[4] T. Katayama, Y. Suzuki, H. Awano, Y. Nishihara, and N. Koshizuka, Phys. Rev. Lett. **60**, 1426 (1988).
[5] W. Reim and D. Weller, Appl. Phys. Lett. **53**, 2453 (1988).
[6] L. Y. Chen, W. A. McGahan, Z. S. Shan, D. J. Sellmyer, and J. A. Woollam, Proc. MRS Symp. **150**, 109 (1989).
[7] W. A. McGahan, L. Y. Chen, Z. S. Shan, D. J. Sellmyer, and J. A. Woollam, Appl. Phys. Lett. **55**, 2479, 1989.
[8] A. V. Sokolov, *Optical Properties of Metals* (Elsevier, New York, 1967), Pt. II.
[9] M. J. Freiser, IEEE Trans. Magn. **MAG-4**, 152 (1968).
[10] P. N. Argyres, Phys. Rev. **97**, 334 (1955).
[11] J. L. Erskine and E. A. Stern, Phys. Rev. B **8**, 1239 (1973).
[12] J. H. Weaver, Phys. Rev. B **11**, 1416 (1975).
[13] P. G. van Engen, K. H. J. Buschow, R. Jongebreur, and M. Erman, Appl. Phys. Lett. **42**, 202 (1983).
[14] P. A. M. van der Heide, W. Baelde, R. A. de Groot, A. R. de Vroomen, P. G. van Engen, and K. J. Buschow, J. Phys. F **15**, L75 (1985).
[15] D. E. Aspnes, E. Kinsbron, and D. D. Bacon, Phys. Rev. B **21**, 3290 (1980).
[16] M. Guerrisi and R. Rosei, Phys. Rev. B **12**, 557 (1975).
[17] L. Y. Chen and D. W. Lynch, Phys. Status Solidi **148**, 387 (1988).
[18] R. A. de Groot, F. M. Mueller, P. G. van Engen, and K. H. J. Buschow, J. Appl. Phys. **55**, 2151 (1984).
[19] K. Egashira and T. Yamada, J. Appl. Phys. **45**, 3643 (1974).
[20] G. S. Krinchik and V. A. Artem'ev Zh. Eksp. Teor. Fiz. **53**, 1901 (1967) [Sov. Phys. JETP **26**, 1080 (1968)].
[21] P. B. Johson and R. W. Christy, Phys. Rev. B **6**, 4370 (1972).
[22] P. B. Johson and R. W. Christy, Phys. Rev. B **9**, 5056 (1974).
[23] J. Kranz and H. Stremme, IEEE Trans. Magn. **MAG-5**, 453 (1969).
[24] Y. Kozono, M. Komur, S. Narishige, M. Hanazono, and Y. Sugita, J. Appl. Phys. **61**, 4311 (1987).
[25] C. Liu, E. R. Moog, and S. D. Bader, Phys. Rev. Lett. **60**, 2422 (1988).
[26] E. R. Moog, J. Zak, M. L. Huberman, and S. D. Bader, Phys. Rev. B **39**, 9496 (1989).
[27] A. J. Freeman and C. L. Fu, J. Appl. Phys. **61**, 3356 (1987).
[28] H. Ehrenreich and H. R. Philipp, Phys. Rev. **128**, 1622 (1962).
[29] A. J. McAlister and E. A. Atern, Phys. Rev. **132**, 1599 (1963).
[30] P. O. Nilsson, I. Landau, and S. B. M. Hagström, Phys. Rev. B **1**, 498 (1970).
[31] H. J. Hagemann, W. Gudat, and C. Kunz, J. Opt. Soc. Am. **65**, 742 (1975).
[32] W. Reim and D. Weller, IEEE Trans. Magn. **MAG-25**, 3752 (1989).